HEAT TRANSFER MEASUREMENTS ON A SIDEWALL AND BLADE SURFACE OF A LARGE SCALE NGV WITH LEAKAGE FLOW

Axel Dannhauer
Institute of Propulsion Technology
Turbine Technology

German Aerospace Center
37037 Göttingen, Germany

ABSTRACT

In the context of a European research program, intensive investigations have to be enforced, to assist the understanding of flow processes and heat transfers in the endwall region of a stator blade, with additional admission by leakage air. To investigate the stationary heat flux with and without the injection of the leakage air a complex measurement set-up is necessary. Infrared images will be taken at the area of interest while the surface of the test item is appended with electric operated heating foils, which generate a constant heat flux into the main flow. By determining the surface temperature and the additional knowledge of the electric power per unit of the heated surface area, a heat transfer coefficient can be defined. With the additional help of the so-called 'superposition method' it is possible to receive the heat transfer coefficient under isoenergetic and the adiabatic film-cooling effectiveness without the need of special thermodynamic boundary conditions.

INTRODUCTION

Due to the necessity of a working clearance between the tips of rotating blades and the outer casing of a turbomachine, fluid is leaking through this clearance and affects not only the efficiency of the stage but also the mass flow rate. Turbine blades may be shrouded or not, so the leakage processes are quite different for these two cases. For shrouded blades, the leakage path is primarily from leading edge to trailing edge. In the case of unshrouded blades, the leakage flow tends to be driven across the rotor tip by the pressure difference between the pressure and suction sides of the blade. As the leakage flow is ejected from the tip gap into the blade passage, it rolls up into a vortex which interacts with the secondary flow passage vortex to form a region of complex flow.

The accurate prediction of the distribution of leakage air as well as their influence on the surface heat transfer at the sidewall, the blade and the transient area in between is therefore important for the understanding of this flow region.

NOMENCLATURE

a	thermal diffusivity
c_p	specific heat
α	heat transfer coefficient
ρ	density
q	specific heat flux
T	temperature
u	streamwise velocity
ε_M	eddy viscosity
ε_H	eddy diffusivity
Θ	nondimensional temperature
η	film-cooling effectiveness

Subscripts

aw	adiabatic wall
f	film-cooled
iw	isoenergetic wall
iso	isotherm
w	wall
∞	free stream
0	total conditions

1. EXPERIMENTAL APPARATUS

1.1. Wind tunnel

The experiments described in this paper will be performed in the NGG wind tunnel of the DLR in Goettingen (see **Figure 1**). The facility is of the blow-down type with atmospheric inlet. The ambient air enters the cascade shortly after the intake. Downstream of the cascade, the flow passes an adjustable diffusor and the main butterfly valve and enters finally a large vacuum vessel. Due to the low downstream mach number of Ma=0,523, measurement times of at least 20 minutes should be

possible. The measurements have to be carried out with and without a turbulence generator, whereby inlet turbulence levels higher than 10% should be achievable. The turbulent grid consist of perforated rectangular rods, with the possibility of up- and downstream injection of compressed air.

The Leakage air will be ejected approximately 2cm upstream of the entrance level of the cascade under three different geometric configurations.

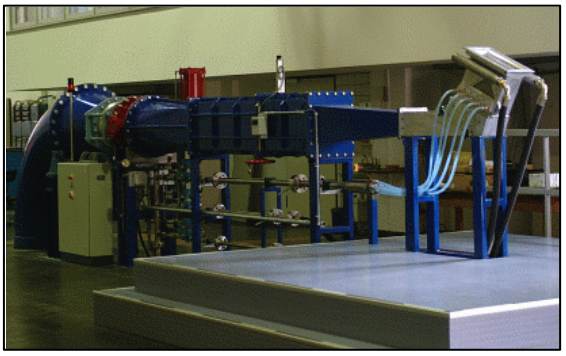

Figure 1: NGG Wind tunnel of the DLR in Goettingen

1.2. Measurement set-up

With the help of an infrared camera, thermographic images will be taken. Since the sidewall as well as the blade have to be examined, the measurements have to be carried out under different observation angles. Therefore the received IR-Pictures have to be transformed later into the coordinate system of the wind tunnel. The surface of the test item will be appended with electric operated heating foils, which generate a constant heat flux. Conduction losses at the sidewall will be measured by heat flux sensors, which are integrated into the sidewall, 5mm under the surface. Equivalent losses at the blade can be minimised by heating the rear side of the blade to reduce the temperature gradient. Additional thermocouples will be used to calibrate the infrared camera. The mass flow of the leakage air will be measured with the help of an orifice flow-meter. All relevant data's of the wind tunnel are recorded simultaneously by our data acquisition (see **Figure 2**).

1.3. Blade construction

At the NGG 3 blades with a chord length of 20cm are arranged as a straight cascade, whereby the middle profile has to be investigated. The measuring blade is constructed in such a way, that the blade profile itself and a part of the sidewall are connected with pins and screws. This facilitates the realisation of the fillet-radius and the coverage of the whole area with electric operated heating foils. Because of the model size as well as the delivery size of the chosen raw material, it is impossible to manufacture the blade and the pertinent region of the sidewall in one piece (see **Figure 3**).

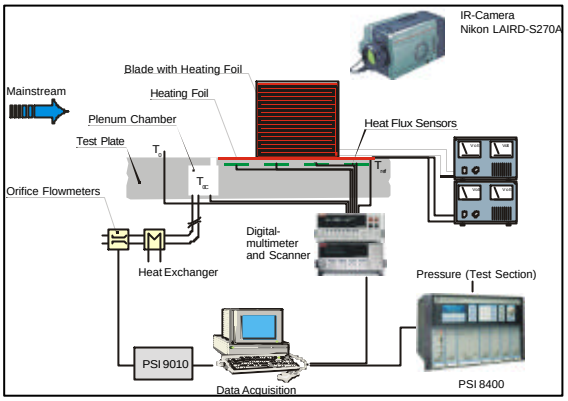

Figure 2: Measurement set-up

Because of the need to reduce heat losses and additionally to resist the high operating temperatures of the heating foils of about 150°C, only two materials remained from the material assortment. These are an epoxy resin (temperature resistant) and Polyether ether ketone (PEEK). PEEK is a semi-crystalline thermoplastic and thermally loadable up to at least 250°C and posses a thermal conductivity of 0,25J/(m·K). To achieve higher mechanical properties a glass-fibre reinforced variant of PEEK will be used. Therefore the thermal conductivity changes to 0,4J/(m·K). The mechanical properties of PEEK are within the range of a Polyamide.

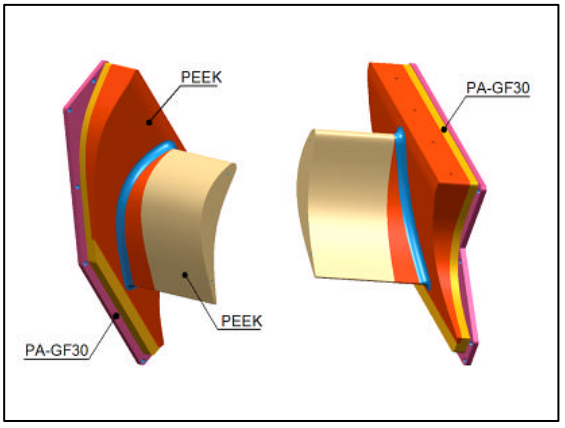

Figure 3: Blade Construction

The temperature resistant epoxy resin is a compound with micro glass bubbles to reduce the thermal conductivity. The problem here is to keep the mixture homogenous during the hardening process. Because the resin needs hours for hardening, the glass bubbles are following the buoyancy force and as a result are concentrated at the surface while the ground consist of pure resin. Due to the schedule these investigations have been cancelled and it was decided to use PEEK for the manufacturing of the measuring blade.

1.3.1. Heating set-up

As already mentioned, the heat-flux is generated by heating foils. These foils consist of a manganin vaporised polyimide foil, whereby the manganin is laid out in form of a meander to ensure an even distribution of the conductive strips. A further polyimide foil is sticked above the conduction layer with the help of an acrylic adhesive. Since the acrylic adhesive starts to decompose at 150°C this temperature also represents the upper limit of the maximal adjustable wall temperature.

In order to be able to receive an ideal of a "black body", the surface of the foils has to be coated with a strongly absorbing colour. Experiences from preceding investigations show that an emissivity of ε=0,99 can be achieved.

Figure 3: Schematic structure of a heating foil

Since also the fillet-radius of our test configuration must be heated, a skilful geometry of the heating foils has to be chosen to cover also the difficult three dimensional shaped regions. Therefore some trials were made, in order to find the optimum solution. Because of the 2D contour in the area of the trailing edge no problems should arise there. At the pressure side the foils can easily be unwinded if the foils are slitted (see **Figure 3**). In contrast the strong curvature within the leading edge area of the suction side might be problematic. We hope to solve this by using several foils. Because of the thickness and the toughness of the foils the success here is dependent on the adhesive with which the foils will be sticked on the surface, since the foils are deformed here. Additionally a special adhesive (ethyl cyanoacrylate) must be used because of the chemical resistance of PEEK.

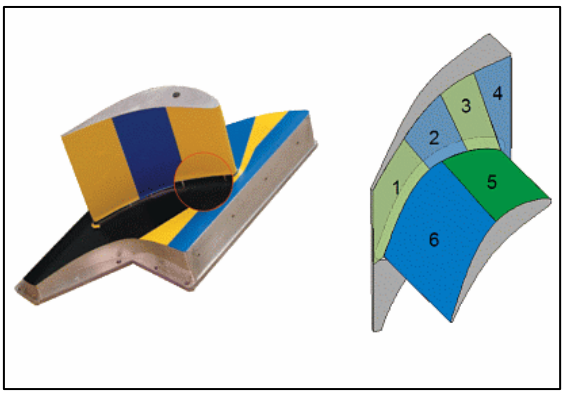

Figure 3: Heating foils are covering the entire range of the test blade

1.3.2. Evaluating of the heating foils

The total operating power of the electrically driven heating foils is calculated with the measured voltage and their resistance. Due to the different layout of the conductive strips, depending on the blades contour, a uniform distribution of the specific power can not be expected.

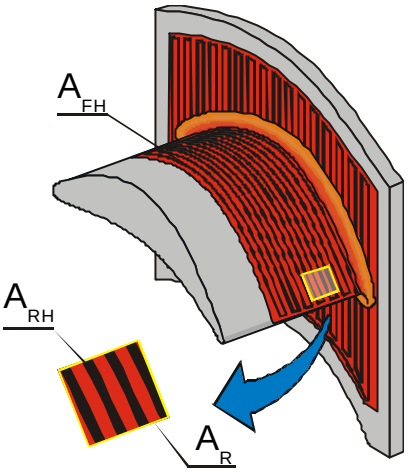

Figure 4: A_{FH} is the total area of conductive stripes, A_R defines the region which has to be observed and A_{RH} is the amount of conductive stripes inside the observed area.

Therefore it makes sense to divide the observed area into small surface elements and evaluate each separately. Thus for every element the appropriate relation between the portion of conductive strips and the element's total area must be found (see **Figure 4**).

$$\Phi = \frac{A_{RH}}{A_{FH}}$$

Multiplying this Quotient with the total operating power one receives the amount of power generated within the area A_R.

$$L_R = L_H \cdot \Phi$$

Finally we receive the specific surface heat flux by dividing L_R by A_R.

$$\Rightarrow \dot{q}_R = \frac{L_R}{A_R}$$

Due to the experience from preceding heat transfer experiments, an average net heat flux of 35kW/m² can be expected.

1.3.3. Carbon conductive ink

If problems will occur in using heating foils in some regions of the fillet, an carbon conductive ink will be used to heat these areas (see **Figure 5**). The paint is based on graphite and can be heated up to a maximum temperature of 120°C. The only disadvantage is the less homogeneous distribution of the heat flux depending on the tolerances in the thickness, but this should be acceptable in case of the small sizes of the problematic areas.

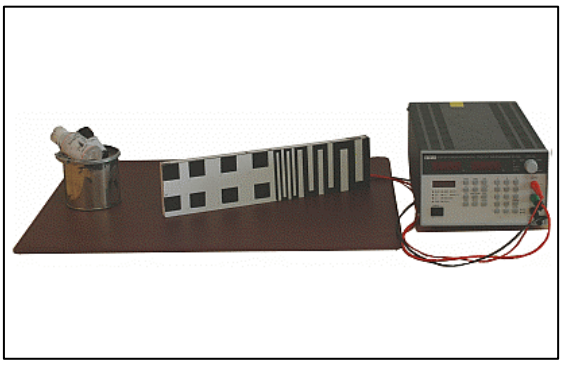

Figure 5: Test set-up for investigations with a carbon conductive ink

1.3.4. Optical access

To accomplish an optical access to the test section at the IR-wavelengths, a ZnS window will be used. Because of the size which would be needed for such a ZnS window, an aluminum sidewall will be constructed, with three different metal inserts in which one ZnS window can be mounted depending on the area of interest. With that construction it is possible to observe a large area without the need of a big, expensive ZnS window (see **Figure 6**).

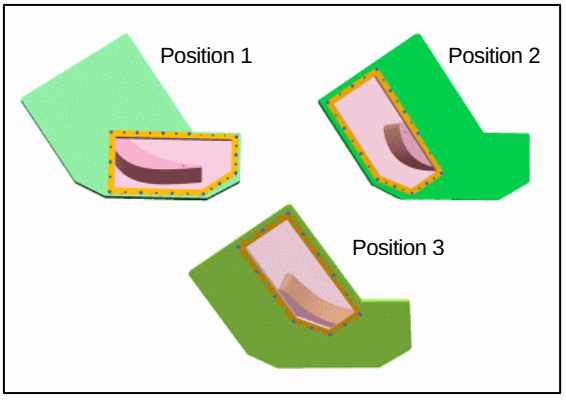

Figure 6: Large observation area without the need of big expensive ZnS window

2. DATA EVALUATION AND PROCEDURES

It is helpful to use the well-known methods from film-cooling examinations, to determine the concentration of leakage air and their influence on the heat transfer. The determination of the so-called film-cooling effectiveness is of large advantage. It is obtained under adiabatic boundary conditions with different temperature differences between leakage air T_{0c} and main flow T_{∞}. The heat transfer downstream of the injection is set to zero (see **Figure 7**).

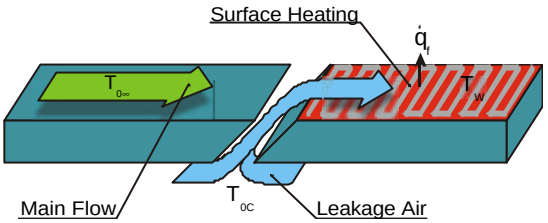

Figure 6: Parameters during a film cooling investigation

The leakage air mixes itself with the main flow according to the aerodynamic conditions in the boundary layer, therefore a resulting temperature is received. In an incompressible flow field this temperature, skilfully normalised, corresponds to the concentration of the leakage air [4]:

$$\eta = \frac{T_{aw} - T_{0\infty}}{T_{0C} - T_{0\infty}} \qquad (2.1)$$

The aerodynamic conditions of the boundary layer are comprised in the standardised temperature h. To examine the change of heat transfer in case of the existence of the leakage flow, additional measurements have to be performed. In order to eliminate the influence of thermal diffusion, the leakage air is ejected with the same temperature as the main flow ($T_{0C} = T_{0\infty}$). A defined heat flux is prescribed downstream the injection point. The resulting heat transfer can be defined as follows.

$$\dot{q}_f = \alpha_{iw} \cdot (T_w - T_{0\infty}) \qquad (2.2)$$

In this equation the heat transfer coefficient α_{iw} denotes the aerodynamic conditions. Here one receives an impression concerning the change of the heat transfer due to the existence of the leakage air.

A film-cooling situation is typically described by three temperatures (T_{0C}, $T_{0\infty}$, T_W). To reduce this problem to two temperatures, the heat transfer can be described in the form:

$$\dot{q}_f = \alpha_{iw} \cdot (T_w - T_{aw}) \qquad (2.3)$$

As mentioned above α_{iw} as well as T_{aw} are functions of the aerodynamic flow field and independent of the temperature boundary conditions.

To receive the favoured parameters η and α_{iw}, without the need of keeping difficult boundary conditions, which can lead to unnecessary errors, the so-called 'superposition method' is applied. This method is based on the acceptance that the energy equation of the boundary layer, as a partial differential equation of second order, is linear in the temperature T(x,y) [1], [2], [3].

$$u\frac{\partial T}{\partial x} + v\frac{\partial T}{\partial y} - (a + \varepsilon_{H,turb.})\frac{\partial^2 T}{\partial y^2} = \frac{u}{\rho \cdot c_p}\left(\frac{\partial p}{\partial x}\right) + \frac{\nu + \varepsilon_{M,turb.}}{c_p}\left(\frac{\partial u}{\partial y}\right)^2 \qquad (2.4)$$

The properties a and ε of the ideal gas are not dependant on the temperature and therefore dependant on the aerodynamic properties alone.

The linearity now permits the superposition of temperature potentials, which are valid under different, simplified boundary conditions.

1. Adiabatic wall:

The leakage air is injected with the temperature $T_{0C} \neq T_{0\infty}$. The heat transfer downstream the outlet is accepted as zero ($\dot{q}_{aw} = 0$).

2. Isoenergetic boundary condition:

The leakage air exits with the same temperature as the undisturbed mainstream: $T_{0C} = T_{0\infty}$, in this case the heat transfer is not equal zero ($\dot{q}_{iw} \neq 0$).

3. Isothermal boundary conditions:

We define $T_{0C} = T_W$. The heat transfer is again not equal zero ($\dot{q}_{iso} \neq 0$).

Summing up the heat flows arising in boundary condition 1 and 2, receives:

$$\dot{q}_{wf} = 0 + \dot{q}_{iw}$$

For the isoenergetic boundary condition 2 the driving temperature difference can be defined as $\Delta T_{iw} = T_{iw} - T_{0\infty}$, the resulting heat flow can be expressed with the help of a heat transfer coefficient:

$$\dot{q}_{wf} = \alpha_{iw} \cdot [T_{iw} - T_{0\infty}] \qquad (2.5)$$

In the adiabatic case, the driving temperature difference for the heat flow would be, $\Delta T_{aw} = [T_{aw} - T_{0\infty}]$. The resulting superimposed driving temperature is therefore $\Delta T_w = \Delta T_{aw} + \Delta T_{iw}$.

Thus equation (2.5) can be rewritten:

$$\dot{q}_{wf} = \alpha_{iw} \cdot (\Delta T_w - \Delta T_{aw}) \qquad (2.6)$$

Combining the boundary conditions 2 and 3, one receives the following heat flow:

$$\begin{aligned} \dot{q}_{wf} &= \dot{q}_{iw} + \dot{q}_{iso} \\ \alpha_f \cdot (T_w - T_{0\infty}) &= \alpha_{iw} \cdot \Delta T_{iw} + \alpha_{iso} \cdot (T_{0c} - T_{0\infty}) \end{aligned} \qquad (2.7)$$

Because of the isoenergetic case ΔT_{iw} can be rewritten: $T_{0c} = T_{0\infty} \Rightarrow \Delta T_{iw} = T_{iw} - T_{0c}$. Without loss of generality one can set $T_{iw} = T_w$. Equation (2.7) can be rewritten thereby as follows:

$$\alpha_f \cdot (T_w - T_{0\infty}) = \alpha_{iw} \cdot (T_w - T_{0c}) + \alpha_{iso} \cdot (T_{0C} - T_{0\infty})$$

$$\frac{\alpha_f}{\alpha_{iw}} = \left(\frac{T_w - T_{oc}}{T_w - T_{0\infty}}\right) + \frac{\alpha_{iso}}{\alpha_{iw}} \underbrace{\left(\frac{T_{0c} - T_{0\infty}}{T_w - T_{0\infty}}\right)}_{=\Theta}$$

$$= 1 + \Theta \underbrace{\left(\frac{\alpha_{iso} - \alpha_{iw}}{\alpha_{iw}}\right)}_{=K}$$

$$\alpha_f = \alpha_{iw}(1 + K \cdot \Theta) \qquad (2.8)$$

If α_f from equation (2.8) is used in (2.7) and if the received expression is compared with equation (2.6), then one receives the following equation:

$$\alpha_{iw} \cdot [T_w - T_{0\infty} + K \cdot T_{0c} - K \cdot T_{0\infty}] =$$

$$\alpha_{iw} \cdot [(T_w - T_{0\infty}) - (T_{aw} - T_{0\infty})]$$

$$K \cdot (T_{0c} - T_{0\infty}) = -T_{aw} + T_{0\infty}$$

$$T_{aw} = T_{0\infty} - K(T_{0c} - T_{0\infty})$$

$$\left[\frac{T_{aw} - T_{0\infty}}{T_{0c} - T_{0\infty}}\right] = -K = \eta$$

With the received definition for -K, equation (2.8) can be rewritten too

$$\alpha_f = \alpha_{iw}(1 - \eta \cdot \Theta) \qquad (2.9)$$

The heat transfer coefficient α_f depends linear on the dimensionless temperature θ (see **Figure 8**).

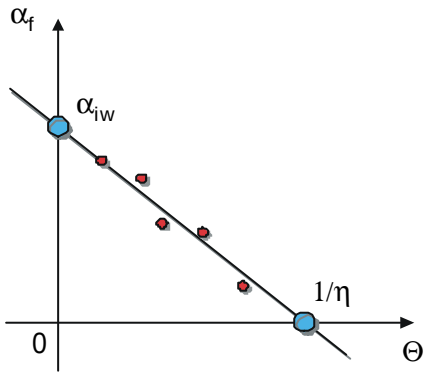

Figure 8: Linear correlation between heat transmission coefficient a_f and temperature Θ.

The intersection of the straight line α_f with the x-axis, corresponds to the reciprocal value of the film-cooling effectiveness and the intersection with the y-axis corresponds to the heat transmission coefficient under isoenergetic boundary conditions [5].

For our measurements this means, that without the necessity of unwieldy boundary conditions e.g. an adiabatic wall or isoenergetic blowing, it is already sufficient to carry out the measurements at arbitrary temperature differences [6].

CONCLUSION

A measurement set-up is presented with which a precise prediction of the stationary surface heat flux in the desired areas is possible. The additional usage of the 'Superposition method' broadens the possibilities of the presented techniques. The additional advantages are:

- Use of arbitrary leakage air temperatures.
- Easy adaptation of arbitrary operating points

Overall the next step is to program a data analysis which automates the transformation of the viewpoints, generate the heat transfer coefficients and interpolate all gathered tensors of the heat transfer coefficients to get the distribution of our desired parameters.

ACKNOWLEDGEMENTS

Main parts of the above research were carried out in the context of the European research program *AITEB* (Aerothermal Investigations on Turbine Endwall and Blades) Work Package 3.

REFERENCES

[1] Eckert, E. R. G.
ANALYSIS OF FILM COOLING AND FULL-COVERAGE FILM COOLING OF GAS TURBINE BLADES
Journal of Engineering for Gas Turbines and Power, 106:pp.206-213, 1984

[2] Eckert, E. R. G.
SIMILARITY ANALYSIS OF MODEL EXPERIMENTS FOR FILM COOLING IN GAS TURBINES
Wärme und Stoffübertragung, 27:pp.217-223, 1992

[3] Shadid, J.N.; Eckert, E. R. G.
THE MASS TRANSFER ANALOGY TO HEAT TRANSFER IN FLUIDS WITH TEMPERATURE-DEPENDENT PRPERTIES
Journal of Turbomachinery, 113:pp.27-33, 1991

[4] Teekaram, A. J. H.; Forth, C. J. P.; Jones, T.V.
COOLING IN THE PRESENCE OF MAINSTREAM PRESSURE GRADIENTS
Journal of Turbomachinery, 113:pp.484-492, 1984

[5] Metzger, D. E.
COOLING TECHNIQUES FOR GAS TURBINE AIRFOIL – A SURVEY
Paper CP-390, S.1/1-1/13, AGARD, 1985

[6] Nicklas, M.
FILM-COOLED TURBINE ENDWALL IN A TRANSONIC FLOW FIELD: PART II – HEAT TRANSFER AND FILM-COOLING EFFECTIVENESS
Paper 2001-GT-0146, SME TURBO EXPO 2001, New Orleans